Energy 65 (2014) 430–440

Contents lists available at ScienceDirect

Energy

journal homepage: www.elsevier.com/locate/energy

Performance comparisons of honeycomb-type adsorbent beds (wheels) for air dehumidification with various desiccant wall materials

Li-Zhi Zhang*, Huang-Xi Fu, Qi-Rong Yang, Jian-Chang Xu

Key Laboratory of Enhanced Heat Transfer and Energy Conservation of Education Ministry, School of Chemistry and Chemical Engineering, South China University of Technology, Guangzhou 510640, China

ARTICLE INFO

Article history:
Received 24 July 2013
Received in revised form
3 October 2013
Accepted 15 November 2013
Available online 15 December 2013

Keywords:
Honeycomb adsorbent bed
Desiccant wheels
Solid desiccant
Dehumidification
Materials
Modeling

ABSTRACT

This study aims at comparing the performance of honeycomb type adsorbent beds (or desiccant wheels) for air dehumidification with various solid desiccant wall materials, from a viewpoint of system operation. A mathematical model is proposed and validated to predict the cyclic behaviors of the cycling beds or wheels. The influences of regeneration air temperature, process air temperature, and humidity on the coefficient of performance (*COP*), specific dehumidification power (*SDP*) and dehumidification efficiency (ε_d) are predicted with various desiccant wall materials. Totally ten most commonly used desiccant materials are considered, with different adsorption and thermophysical properties. It is found that of the 10 materials, the silica gel 3A and silica gel RD perform better than other desiccants for air dehumidification under typical working conditions and driven by low grade waste heat. The results provide some insights and guidelines for the design and optimization of honeycomb type adsorption beds or desiccant wheels.

1. Introduction

Air-conditioning in hot and humid environment is an essential part for human health and comfort [1–3]. Humidity control is a major task for air conditioning [4]. Outside air humidity stays above 80–90% continuously for a dozen of days in subtropical regions like South China. It is necessary to dehumidify fresh air before it can be supplied to buildings. Air dehumidification has played a crucial role in modern air conditioning industry which tends to separate the treatment of latent load from sensible load [5]. In fact, air dehumidification accounts for 40–60% of the cooling load for air conditioning in hot and humid regions like Southern China.

Solid desiccants, either in the form of cycling honeycomb beds or revolving desiccant wheels, are the most common technology for air dehumidification. Various desiccants have been analyzed. Ng et al. [6] investigated the adsorption isotherm characteristics of silica gel–water pair. Tashiro et al. [7] assessed the performance of three types of silica gel, a zeolite with various molar ratios of Si/Al, and an activated carbon with silica gel added. Nakabayashi et al. [4] improved the water vapor adsorption ability of a natural mesoporous material, Wakkanai siliceous shale, by impregnating it with chloride salts. Zhang et al. [8] studied the silica gel-calcium chloride composite desiccant wheel. It was found that the new composite desiccants can be effectively used in a rotary wheel dehumidifier and the performance was improved. Chan et al. [9] predicted the performance of a new zeolite 13X/$CaCl_2$ composite adsorbent for adsorption cooling systems. Yadav and Bajpai [10] compared the regeneration performance of silica gel, activated alumina, and activated charcoal by an evacuated solar air collector and air dehumidification system. It is easy to conclude that though many desiccants have been analyzed, they were investigated only as a “raw material”, rather than as a “system”. Previous work concentrated on the analysis of adsorption isotherms of various desiccants, by neglecting their performance in a real desiccant system. It should be noted that the real performance should be analyzed from the viewpoint of a “system”. The performance of a desiccant system is related not only to the basic adsorption properties of the raw materials, but also to the operating conditions and the heat and mass transfer properties in the beds. Different materials, even having the same adsorption capabilities, may have different performances if they are made into adsorbent beds and operated under real working conditions. Therefore, it is more significant to compare these desiccants from the viewpoint of a “system”.

* Corresponding author. Tel./fax: +86 20 87114268.
E-mail address: Lzzhang@scut.edu.cn (L.-Z. Zhang).

0360-5442/$ – see front matter © 2013 Elsevier Ltd. All rights reserved.
http://dx.doi.org/10.1016/j.energy.2013.11.042

Nomenclature

A_{tot}	the total heat and mass transfer area in adsorbent bed (m^2)
C	constant in sorption curve
COP	coefficient of performance
c_p	specific heat (kJ kg^{-1} K^{-1})
D	diffusivity (m^2 s^{-1})
D_h	hydrodynamic diameter of a channel (m)
f	desiccant content
H	height of the solid adsorption bed (m)
H_{sc}	height of a single sinusoidal channel (m)
h	convective heat transfer coefficient (kW m^{-2} K^{-1})
k	convective mass transfer coefficient (ms^{-1})
k'_m	internal mass transfer coefficient based on humidity difference (s^{-1})
k_m	internal mass transfer coefficient of adsorbents (s^{-1})
K_p	partition coefficient [(kg water/kg material)/(kg vapor/kg air)]
P_{heater}	maximum power of the regeneration heater (kW)
L	length of the solid adsorbent bed (m)
L_v	latent heat of water vapor (kJ kg^{-1})
$\dot{m}$	mass flow rate of process or regenerating air stream (kg s^{-1})
m_d	mass of the bed (kg)
n	number of ducts in a bed
Nu	Nusselt number
q_{st}	adsorption heat (kJ kg^{-1})
SDP	specific dehumidification power (kg kg^{-1} h^{-1})
Sh	Sherwood number
t	time (s)
T	temperature (K)
u_a	bulk air velocity (ms^{-1})
$u_{p,\,i}$	process air inlet velocity (ms^{-1})
$u_{r,\,i}$	regeneration air inlet velocity (ms^{-1})
W	width of the solid adsorbent bed (m)
W_{sc}	width of a single sinusoidal channel (m)
w	water uptake in adsorbent (kg water/kg dry adsorbent)
w_{max}	maximum water uptake of adsorbent (kg kg^{-1})
x	axial coordinate (m)
z	thickness coordinate (m)

Greek letters

ϕ	relative humidity
λ	thermal conductivity (kW m^{-1} K^{-1})
ε_d	dehumidification efficiency
ε_t	total porosity
ρ	density (kg m^{-3})
δ	half thickness of solid wall (m)
ω	humidity ratio (kg moisture/kg dry air)

Subscripts

a	air
ad	adsorption
cyc	cycle
d	desiccant wall
de	desorption
eq	equilibrium
gf	glass fiber paper
i	inlet
ide	ideal
max	maximum
min	minimum
o	outlet
p	process air
r	regeneration air
s	surface, solid
th	thermal
v	vapor
w	water
z	thickness

In this paper, the dehumidification performances with ten kinds of solid desiccants, namely the silica gel B (developed in our Lab), silica gel 3A, silica gel RD, silica gel/LiCl (10 wt.%) composite, silica gel/$CaCl_2$ (27.3 wt.%) composite, zeolite 5A, zeolite 13X, zeolite 13X/$CaCl_2$ (41.5mol.%) composite, $CaCl_2$ and LiCl, as the wall materials for honeycomb-type adsorbent beds, are compared.

The physical structures of silica gels B, 3A and RD are presented in Table 1. From Table 1, we can see that the specific surface area of silica gel B is less than that of silica gel 3A and RD, but the average pore diameter and porous volume are larger than that of silica gel 3A and RD. These differences will affect their adsorption equilibrium, and result in a different dehumidification performance indirectly.

Lithium chloride and calcium chloride have a higher hygroscopic capacity, but the lyolysis phenomenon, which leads to the loss of desiccant materials and may reduce the performance, often takes place after the formation of solid crystalline hydrate [11]. So the weight or molar loading of lithium chloride or calcium chloride for the silica gel/LiCl, silica gel/$CaCl_2$ and zeolite 13X/$CaCl_2$ composite adsorbent should be considered. According to references [11,12,9], in this paper, we choose 10 wt.% as the weight loading for silica gel/LiCl composite, 27.3 wt.% for silica gel/$CaCl_2$ and 41.5 mol.% as the molar mass loading for zeolite 13X/$CaCl_2$. These concentrations are the best feasible choices and were tested. Their thermophysical properties are available.

To predict the dehumidification performance, a one-dimensional, transient heat and mass transfer model [13] is proposed in this paper. The advantages of such a model lay in the fact that it considers the dominant mechanisms for heat conduction and mass diffusion in the wall thickness, while using the air side Nusselt and Sherwood numbers developed specially for the adsorbent ducts. With the validated model, the dehumidification performances of cycling honeycomb adsorbent beds with these materials are compared.

Table 1
Physical structures of silica gels B, 3A and RD.

	Specific surface area (m^2 g^{-1})	Porous volume (ml g^{-1})	Average pore diameter (nm)	Ref.
Silica gel B	476	0.61	4.78	–
Silica gel 3A	606	0.45	3.0	[6]
Silica gel RD	650	0.35	2.1	[6]

2. Mathematical model

2.1. The system and the test rig

A honeycomb type adsorbent bed consisted of numerous flow channels as shown in Fig. 1 is fabricated in our laboratory. A series

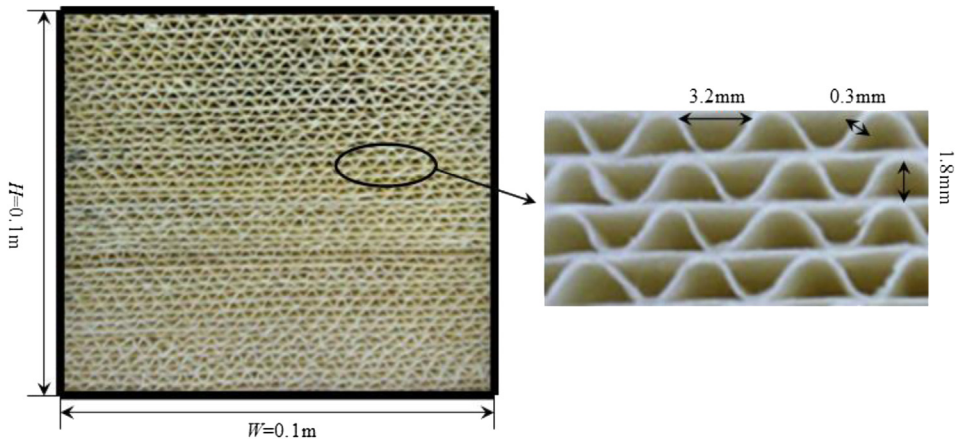

Fig. 1. Geometry of the honeycomb type adsorbent bed for air dehumidification.

of parallel sinusoidal straight ducts are packed together to form the bed. The bed is made with glass fiber paper impregnated with desiccant materials. The honeycomb walls contain 80% of desiccant materials (f = 0.8). The pitch of the sinusoidal channel is 3.2 mm × 1.8 mm with a half thickness of wall of 0.15 mm. A representative duct, as shown in Fig. 2, is selected as the calculation domain, comprising of an air duct and two neighboring walls.

The honeycomb type adsorbent bed is used for intermittent air dehumidification. The bed is switched between adsorption and regeneration modes, as shown in Fig. 3. Fig. 3(a) shows the real picture of the test rig, and Fig. 3(b) shows the schematic of the system. As seen, the system is comprised of two fans, the ductwork, a heater, four valves, a bed, and sensors. When Valves 2, 4 are opened, and Valves 1, 3 are closed, heated regeneration air is pumped to the bed. It works in regeneration mode. The bed is heated and the adsorbed water in the adsorbent is driven away. When Valves 1, 3 are opened, and Valves 2, 4 are closed, process air is pumped to the bed, the adsorbents in the bed are cooled and moisture in the air stream is removed by the adsorbent walls. This is called the adsorption mode. As the adsorption mode goes on, the adsorbent becomes saturated. Regeneration mode is required again, and a new cycle begins. As seen, the bed works alternately between regeneration and adsorption modes.

2.2. Governing equations

The mathematical model and the numerical analysis are based on the following assumptions:

(1) The channels are equally and uniformly distributed throughout the bed;
(2) The thermodynamic properties in the solid are constants, and uniform;
(3) The air flow is one-dimensional;
(4) For air stream, the axial heat conduction and water vapor diffusion are neglected;

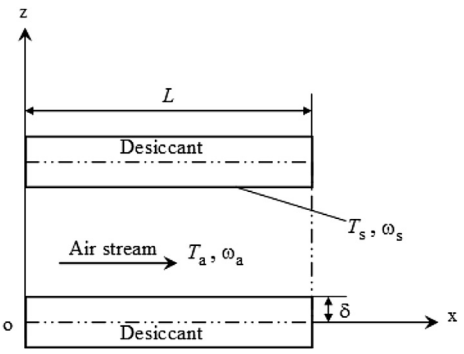

Fig. 2. Calculation domain of a channel in the adsorbent bed.

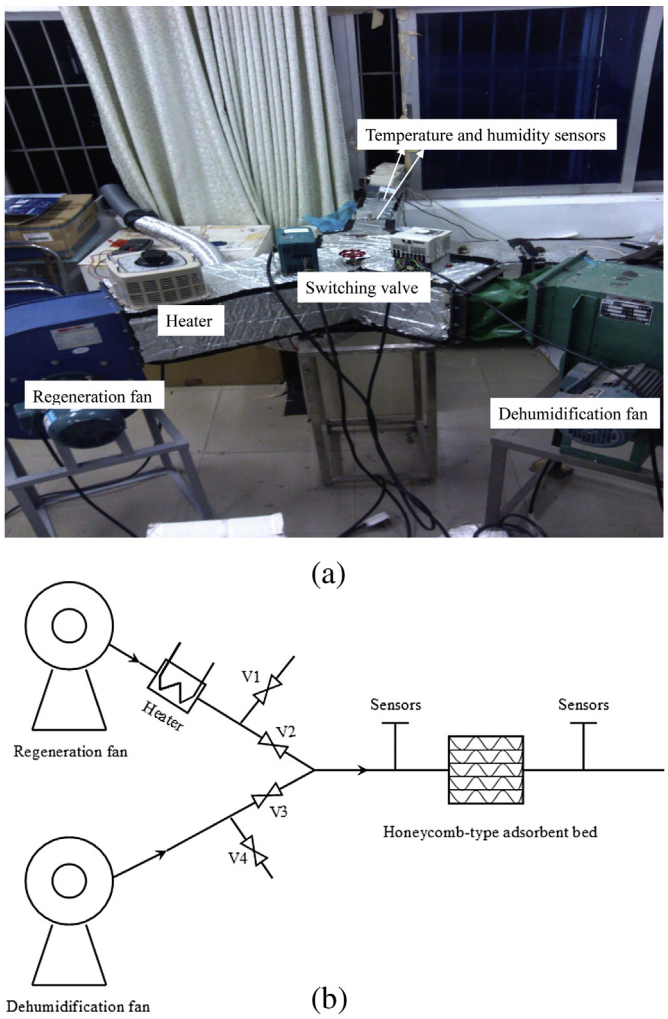

Fig. 3. Experimental set-up for air dehumidification with the honeycomb type adsorbent bed: (a) photo of the test rig, (b) schematic of the test rig.

(5) For solid phase, only heat conduction and mass diffusion in wall thickness are considered;

According to these assumptions, the model used in this study is transient and one-dimensional [13]. Because of symmetry, the mid-plane of the channel can be considered to be adiabatic, and a half-size channel surrounded by the dashed lines is used as the calculation domain, as already shown in Fig. 2.

Energy and mass conservation in the air stream are written as

$$\frac{1}{u_a}\frac{\partial T_a}{\partial t}+\frac{\partial T_a}{\partial x}=\frac{4h}{\rho_a u_a D_h c_{pa}}(T_s-T_a) \tag{1}$$

$$\frac{1}{u_a}\frac{\partial \omega_a}{\partial t}+\frac{\partial \omega_a}{\partial x}=\frac{4k}{u_a D_h}(\omega_s-\omega_a) \tag{2}$$

where u_a is the air bulk velocity (ms^{-1}), T_a and ω_a are temperature (°C) and humidity ratio ($kg\ kg^{-1}$) of air respectively, t is time (s), x is axial coordinate (m), D_h is the hydrodynamic diameter of the channel (m), c_{pa} is the specific heat ($kJ\ kg^{-1}\ K^{-1}$) and ρ is the density ($kg\ m^{-3}$), h and k are the convective heat transfer ($kW\ m^{-2}\ K^{-1}$) and mass transfer (ms^{-1}) coefficients between the air stream and the solid surface, respectively. Heat and mass transfer coefficients are calculated by

Nusselt number

$$Nu=\frac{hD_h}{\lambda_a} \tag{3}$$

Sherwood number

$$Sh=\frac{kD_h}{D_{va}} \tag{4}$$

where λ_a and D_{va} are heat conductivity ($kW\ m^{-1}\ K^{-1}$) and moisture diffusivity in air ($m^2\ s^{-1}$), respectively. For our system, the Reynolds number in the air flow channels in the adsorbent bed is less than 2300. It is a fully developed laminar flow. For such fully developed laminar flow, the Nu and Sh are constants, varying only with the shape and the aspect ratio of the channel. In this paper, the channel has a sinusoidal shape, with a height of 1.8 mm and a width of 3.2 mm, so the Nu and Sh are selected to be 2.2 and 2.05 [13,14], respectively.

Energy conservation of the desiccant material is written as

$$\rho_d c_{tot}\frac{\partial T}{\partial t}=\frac{\partial}{\partial z}\left(\lambda_d\frac{\partial T}{\partial z}\right)+q_{st}\rho_d\frac{\partial w}{\partial t} \tag{5}$$

where ρ_d is the density of the desiccant wall ($kg\ m^{-3}$), λ_d is the thermal conductivity of the wall ($kW\ m^{-1}\ K^{-1}$), w is the water content in the wall ($kg\ kg^{-1}$), z is the coordinate in the thickness (m), q_{st} is the adsorption heat ($kJ\ kg^{-1}$), c_{tot} is the total heat capacity of wet desiccant wall, which includes three parts: dry glass fiber paper, dry desiccant and adsorbed water and is calculated by

$$c_{tot}=(1-f)c_{pgf}+f\left(c_{pd}+wc_{pw}\right) \tag{6}$$

where c_{pgf}, c_{pd} and c_{pw} are the specific heat ($kJ\ kg^{-1}\ K^{-1}$) of dry glass fiber paper, dry desiccant and liquid water, respectively. The heat capacity of moist air in the solids is neglected. In this paper, the one-dimensional model is used. This is because the length scale in flow direction ($L=0.1$ m) is much larger than that in wall thickness ($\delta=0.15$ mm). The heat conduction and moisture diffusion in solid along x-direction is several magnitudes lower than those in thickness and can be neglected. In fact the current author has developed the 2-D model early in 2002 [15]. Later we noticed this part can be neglected for small thickness wheel walls. An another benefit is that 1-D model is quicker in solution.

Even with this 1-D model, the temperature change in the solid along air flow can be reflected. This is because the air temperature changes axially. Due to coupling, the solid temperature also changes with flow.

The mechanisms of moisture diffusion in the desiccant are very complicated. Two phases of water, namely, gas and adsorbed state, co-exist and diffuse in the pores of the solid. There are three dominant diffusion mechanisms [16]: surface diffusion, ordinary diffusion, and Knudsen diffusion. The equivalent moisture diffusivity in solids, based on air humidity ratio differences, is denoted by D_{vs} ($m^2\ s^{-1}$). The moisture conservation in the solid can be expressed as

$$\varepsilon_t\rho_a\frac{\partial \omega}{\partial t}+\rho_d\frac{\partial w}{\partial t}=\rho_a\frac{\partial}{\partial z}\left(D_{vs}\frac{\partial \omega}{\partial z}\right) \tag{7}$$

where ε_t is the total porosity of the desiccant. The right hand side of Eq. (7) is the moisture transfer by effective diffusion. In our earlier work [15], we used both diffusion in gas phase and in adsorbed phase. Later we found it too complicated for engineering applications, since it's difficult to differentiate among different mechanisms. So here we summarize all the diffusion mechanisms in this effective D_{vs}. This is in fact an "effective diffusivity" which includes all the mechanisms. The driving force is humidity difference, rather than non-measurable water uptake. The effective diffusivity values can be measured by the FLEC system [17] in our Lab, which is based on the permeation tests of moisture. The detailed values of several common materials are described in Ref. [13].

Considering non-equilibrium adsorption, the adsorption rate is governed by Ref. [18]

$$\frac{\partial w}{\partial t}=k_m(w_{eq}-w) \tag{8}$$

where k_m is termed as the internal mass transfer coefficient (s^{-1}) of adsorbents, which can be evaluated by adsorption curves. w_{eq} is the equilibrium water content in solid at temperature T and humidity ratio ω.

The equilibrium water uptake in the desiccant can be expressed by a general sorption curve as

$$w_{eq}=\frac{fw_{max}}{1-C+C/\phi} \tag{9}$$

where this sorption curve directly links water content to ϕ, a variable that can be directly measured.

Equation (8) can be re-written as

$$\frac{\partial w}{\partial t}=k'_m(\omega_{eq}-\omega) \tag{10}$$

$$k'_m=K_p k_m \tag{11}$$

where K_p is partition coefficient expressed as $w_{eq}=K_p\omega$, which is a linear approximation of the relation between equilibrium adsorption uptake and humidity. It can be estimated by Eq. (9).

Using Clapeyron equation to represent the saturation vapor pressure and assuming a standard atmospheric of 101,325 Pa gives the relation between humidity and relative humidity as

$$\frac{\phi}{\omega} = 10^{-6}e^{5294/T} - 1.61\phi \tag{12}$$

where T is in K.

2.3. Initial and boundary conditions

Initial conditions and boundary conditions for air steam.

For dehumidification period, $0 \le t < t_{ad}$, the inlet conditions:

$$\begin{cases} T_a|_{x=0} = T_{p,\,i} \\ \omega_a|_{x=0} = \omega_{p,\,i} \end{cases} \tag{13}$$

For regeneration period, $t_{ad} \le t < t_{cyc}$, the inlet conditions:

$$\begin{cases} T_a|_{x=0} = T_{r,\,i} \\ \omega_a|_{x=0} = \omega_{r,\,i} \end{cases} \tag{14}$$

Boundary conditions for the solid phase:

$$\left.\frac{\partial T}{\partial x}\right|_{x=0} = \left.\frac{\partial T}{\partial x}\right|_{x=L} = \left.\frac{\partial T}{\partial z}\right|_{z=0} = 0 \tag{15}$$

$$\left.\frac{\partial \omega}{\partial x}\right|_{x=0} = \left.\frac{\partial \omega}{\partial x}\right|_{x=L} = \left.\frac{\partial \omega}{\partial z}\right|_{z=0} = 0 \tag{16}$$

$$-\lambda_d\left.\frac{\partial T}{\partial z}\right|_{z=\delta} = h(T-T)_a \tag{17}$$

$$-D_{vs}\left.\frac{\partial \omega}{\partial z}\right|_{z=\delta} = k(\omega-\omega_a) \tag{18}$$

where δ is the half thickness of the channel wall (m), and L is the length of the channel (m).

2.4. Performance indices

In this paper, three indices (including the *COP* (coefficient of performance), *SDP* (specific dehumidification power) and ε_d) are defined to assess the dehumidification performance of various solid desiccants. The adsorption time for every single duct is t_{ad}, and the desorption time is t_{de}, so the cycle time $t_{cyc} = t_{ad} + t_{de}$. The mean outlet temperature and humidity for the process air ($0 \le t < t_{ad}$) can be calculated by the integration of the outlet values over time t,

$$\overline{T}_{p,o} = \frac{\int_0^{t_{ad}} T_{p,o}\mathrm{d}t}{t_{ad}} \tag{19}$$

$$\overline{\omega}_{p,o} = \frac{\int_0^{t_{ad}} \omega_{p,o}\mathrm{d}t}{t_{ad}} \tag{20}$$

The mean outlet temperature and humidity for the regeneration air ($t_{ad} \le t < t_{cyc}$) are calculated by

$$\overline{T}_{r,o} = \frac{\int_{t_{ad}}^{t_{cyc}} T_{r,o}\mathrm{d}t}{t_{de}} \tag{21}$$

$$\overline{\omega}_{r,o} = \frac{\int_{t_{ad}}^{t_{cyc}} \omega_{r,o}\mathrm{d}t}{t_{de}} \tag{22}$$

For cooling cycle, the thermal coefficient of performance (COP_{th}) is defined with the effective cooling capacity (it's the enthalpy change of the process air from inlet state to outlet state) divided by the regeneration heat consumption [19]. For air dehumidification system, in this paper, the dehumidification coefficient of performance (*COP*) of the adsorbent bed is particularly defined. The parameter reflects the dehumidification performance and energy consumption synthetically, and can be expressed by:

$$COP = \frac{\dot{m}_p L_v(\omega_{p,i} - \overline{\omega}_{p,o})}{\dot{m}_r c_{pa}(T_{r,i} - \overline{T}_{r,o})} \tag{23}$$

where the denominator is the regeneration heat consumption (the input energy) during regeneration process; and the numerator is the effective dehumidification energy (the useful energy) during dehumidification process, it reflects the dehumidification capacity indirectly. So for air dehumidification system, the *COP* is particularly defined, we just consider the effective latent heat change of process air. $\dot{m}_p$ is the mass flow rate of process air stream (kg s^{-1}), $\dot{m}_r$ is the mass flow rate of regeneration air stream (kg s^{-1}), L_v is latent heat of water vapor (kJ kg^{-1}).

The specific dehumidification power (*SDP*) for every complete cycle (kg kg^{-1} h^{-1}) is expressed by:

$$SDP = \frac{\dot{m}_p(\omega_{p,i} - \overline{\omega}_{p,o})t_{ad}3600}{m_d t_{cyc}} \tag{24}$$

The dehumidification efficiency (ε_d) for every complete cycle can be written as:

$$\varepsilon_d = \frac{\omega_{p,i} - \overline{\omega}_{p,o}}{\omega_{p,i} - \omega_{p,o,ide}} \tag{25}$$

where $\omega_{p,o,ide}$ (kg kg^{-1}) is the ideal outlet humidity ratio for process air. It is the equilibrium humidity ratio of material at adsorption temperature $T_{p,i}$, and minimum water uptake w_{min}, which itself is determined by the adsorption isotherm at temperature $T_{r,i}$, and humidity $\omega_{r,i}$ of regeneration air.

2.5. Numerical solution

The one-dimensional heat and mass transfer equation of the desiccant are numerically solved by finite difference method [15]. Because the equations are strongly coupled and non-linear, iterations are necessary to get converged values for each time step. The whole calculating domain is divided into a number of equal-step discrete elements. Each element is identified as a control volume by a nodal point. The numbers of nodes are: 60 in axial, 20 in thickness, and 120 in time. The temperature and humidity fields in the solid and in the air stream are calculated at each time interval. Then the mean outlet values are obtained by the integrations of outlet values over the adsorption or desorption period. At last, the performance indices can be calculated.

3. Result and discussion

3.1. Experimental validation with self-developed desiccant

The model is validated with the self developed desiccant bed and the dehumidification system described in section 2.1. For the

self-made honeycomb bed, the wall material is silica gel B. The fabrication process is: (1) Fiber glass paper is soaked with water glass solution. (2) They are then corrugated and stacked together to form a honeycomb structure. (3) The structure is immersed in a H_2SO_4 solution bath. (4) After some period, it is picked up and dried at a certain temperature for several hours. (5) Finally the honeycomb bed is formed. The properties of the bed are measured and are listed in Table 2. Also listed in Table 2 are nine other typical desiccants for numerical comparisons later. Their properties are taken from references. The structural and operating parameters for the bed are listed in Table 3. The whole test rig is placed in a constant temperature and constant humidity chamber, so inlet humidity and temperature for the process stream can be adjusted stably. The temperature, humidity and flow rates to and from the adsorbent bed are measured with sensors and are recorded with time. Measurement uncertainties are: temperature, ±0.1 °C, relative humidity, ±2%, and velocity ±3%. The measured data are compared with the calculated data with the model.

Four inlet operating conditions are used for the process air (the adsorption air): hot and humid, hot and dry, cool and humid, and cool and dry conditions, as listed in Table 4. The inlet humidity ratios for the regeneration air are the same as those for the process air. The inlet temperatures and flow rates for the regeneration air are different from the process air.

Fig. 4 shows the variations of the outlet air temperature and humidity with time under hot and humid operating conditions for the fresh process air and the regeneration air. Cyclic behaviors are observed both for temperature and for humidity variations. For each adsorption stage in a cycle, the outlet temperature decreases fast at the beginning. This is the isosteric cooling period where little moisture is adsorbed. Then the outlet temperature decreases faster and much moisture is adsorbed. This is the adsorption period. For each regeneration stage in a cycle, the outlet temperature rises steadily at first and little moisture is regenerated. This is the isosteric heating period. Then the outlet temperature rises sharply and humidity drops sharply. This is the desorption period where the temperature rises quickly with less water remained in the bed. The behaviors have been investigated for a desiccant wheel [15]. The maximum differences between calculated values and tested values are 9.8% for temperature and 12% for humidity, respectively. Generally, the calculated results show good agreement with the experimental results, so the model can be used to predict the performance of adsorbent beds.

3.2. Comparisons of performances with different materials

Performances of the adsorbent beds are influenced not only by the adsorption isotherms, but also by many operating factors. The ten commonly used desiccant materials listed in Table 2 are modeled with the mathematical model developed above. The operating and structural parameters are the same, as listed in Table 3. The resulting performances are compared for the four operating conditions listed in Table 4.

Table 3
Structural and operating parameters for the adsorbent bed.

Symbol	Unit	Value
A_{tot}	m^2	2.29
L	m	0.1
L_v	kJ kg^{-1}	2258
W	m	0.1
H	m	0.1
W_{sc}	mm	3.2
H_{sc}	mm	1.8
δ	mm	0.15
D_{va}	$m^2\ s^{-1}$	2.82×10^{-5}
D_{vs}	$m^2\ s^{-1}$	3.5×10^{-7} [17]
k'_m	s^{-1}	0.32 [13]
P_{heater}	kW	2.1
$u_{p,\ i}$	ms^{-1}	1.0
$u_{r,\ i}$	ms^{-1}	1.3
t_{cyc}	min	10
t_{ad}	min	5
t_{de}	min	5
Nu		2.2
Sh		2.05
f		0.8
n		2800

Table 4
Four inlet conditions for the process air.

	T/°C	ϕ/%	ω/(kg kg^{-1})
Hot and humid	30	85	0.02325
Hot and dry	30	20	0.00532
Cool and humid	20	85	0.01259
Cool and dry	20	30	0.00439

3.2.1. Hot and humid conditions

Figs. 5–7 show the calculated *COP*, *SDP* and ε_d with different regeneration temperatures under hot and humid operating conditions for the process air.

Fig. 5 shows that the regeneration temperature has little impact on the *COP* under this operating condition. The reason is that the higher the regeneration temperature is, the larger the energy input is, and the larger the useful energy output is. Energy use and energy generation are in phase. Besides, the highest *COP*s (with values equal to 0.8) are obtained for Silica gels 3A and RD, while the lowest *COP*s (with values equal to 0.45) are obtained for zeolites 5A and 13X. The main reason is that the adsorption heat of zeolites 5A and

Table 2
Thermophysical properties of various solid desiccants.

	c_p (kJ $kg^{-1}\ K^{-1}$)	λ (k $Wm^{-1}\ K^{-1}$)	ρ (kg m^{-3})	w_{max}(kg kg^{-1})	q_{st} (kJ kg^{-1})	ε_t	Refs	C	m_d (kg)
Silica gel B[a]	0.921	1.98×10^{-4}	790	0.40	2362	0.50	–	1.1	0.231
Silica gel 3A	0.921	1.74×10^{-4}	770	0.35	2380	0.56	[6]	1.1	0.225
Silica gel RD	0.921	1.98×10^{-4}	800	0.37	2370	0.44	[6]	1.1	0.234
Silica gel/LiCl	0.921	2.39×10^{-4}	875	0.60	2476	0.36	[11,20]	1.5	0.256
Silica gel/$CaCl_2$	0.866	3.20×10^{-4}	976	0.55	2620	0.41	[12,21,22]	1.3	0.285
Zeolite 5A	0.950	2.09×10^{-4}	680	0.19	3974	0.32	–	0.2	0.199
Zeolite 13X	0.950	2.09×10^{-4}	650	0.22	3843	0.35	[23]	0.2	0.190
Zeolite 13X/$CaCl_2$	0.836	2.00×10^{-4}	1100	0.46	3398	0.30	[9]	0.5	0.322
$CaCl_2$	0.620	2.10×10^{-4}	2150	0.33	3675	0.01	[23,24]	1.0	0.628
LiCl	1.132	6.50×10^{-4}	2068	0.43	2957	0.08	[11,24]	1.0	0.605

Remark: when the lyolysis phenomenon is not occurred, the largest adsorption capacity (w_{max}) of $CaCl_2$ and LiCl are 0.33 kg kg^{-1} and 0.43 kg kg^{-1}, respectively.
[a] Silica gel B is in-situ developed in our laboratory and is used for tests.

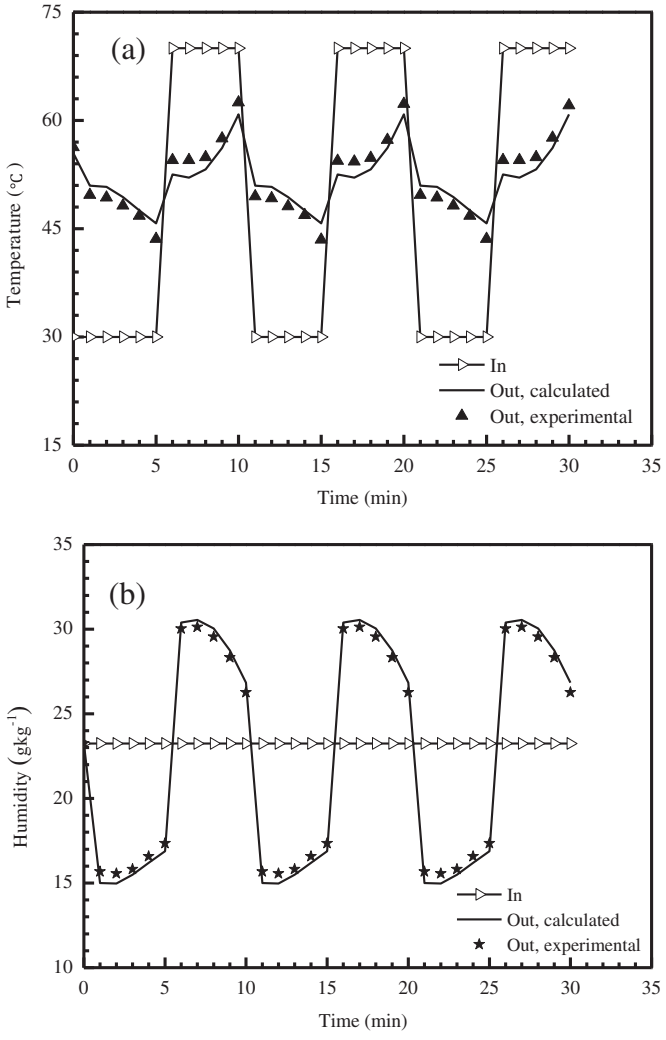

Fig. 4. Variations of the outlet air temperature (a) and humidity (b) with time under hot and humid operating conditions: comparison between experimental data and calculated data ($T_{r,\,i} = 70$ °C, $u_{p,\,i} = 1.0$ m/s, $u_{r,\,i} = 1.3$ m/s). The material used is self-made Silica gel B.

13X are higher than others, so that they need more driving heat to desorb the same amount of water vapor.

The *SDP* increases monotonically with a higher regeneration temperature, as shown in Fig. 6. This is simply because water vapor

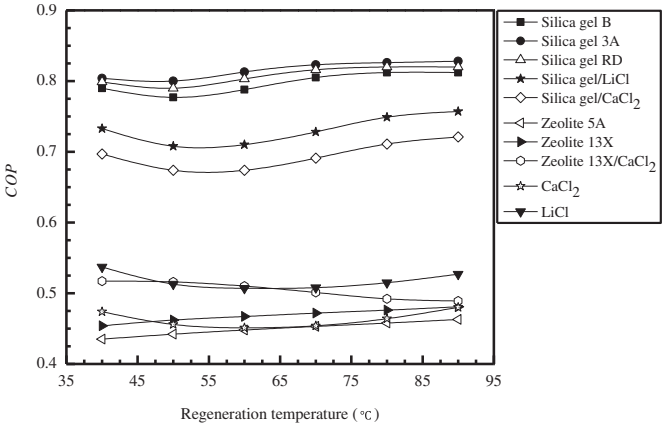

Fig. 5. Effects of regeneration temperature on *COP* under hot and humid operating conditions.

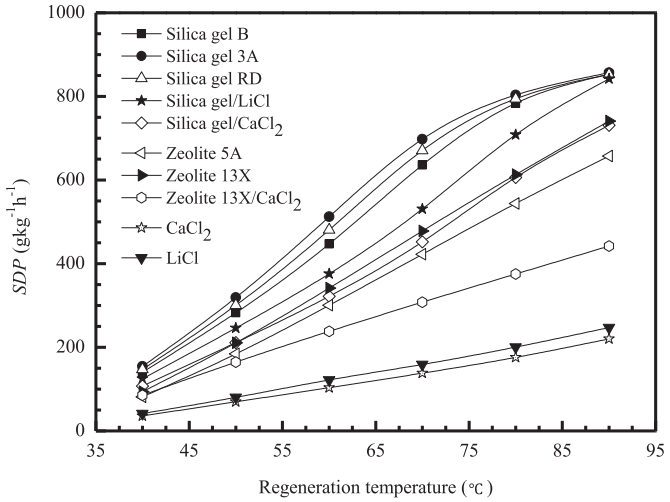

Fig. 6. Effects of regeneration temperature on *SDP* under hot and humid operating conditions.

is desorbed faster at higher desorption temperatures, which then causes more water vapor to be adsorbed during the next adsorption process [25]. It is also found that the *SDP*s of silica gels 3A and RD are higher than others at different regeneration temperatures, while the lowest *SDP*s are obtained for $CaCl_2$ and LiCl. The reason is that the adsorption heat of $CaCl_2$ and LiCl are very high. They are equal to those of zeolites 5A and 13X. Furthermore, the densities of $CaCl_2$ and LiCl are larger, which leads to a larger mass loading (the volume of bed is fixed) than others. From Eq. (24), it can be seen that when the dehumidification amount is almost the same, the larger the mass is, the lower the *SDP* is.

The variations of ε_d with regeneration temperature are shown in Fig. 7. It can be noticed that the ε_d of silica gels B, 3A and RD is higher than others when the regeneration temperature is less than 80 °C. However when the regeneration temperature is $T_{r,i} = 90$ °C, the ε_d of silica gel/LiCl and silica gel/$CaCl_2$ composites reaches the highest values of 46%. Besides, the ε_d of zeolites 5A and 13X is always lower than others at different regeneration temperatures. This is because the maximum equilibrium water content of zeolites 5A and 13X (with values equal to 0.19 kg kg^{-1} and 0.22 kg kg^{-1}, respectively, about 50% of others) is the lowest among various

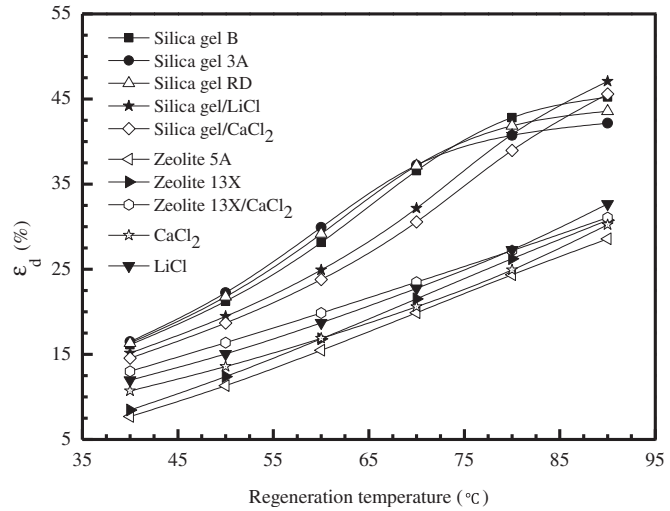

Fig. 7. Effects of regeneration temperature on ε_d under hot and humid operating conditions.

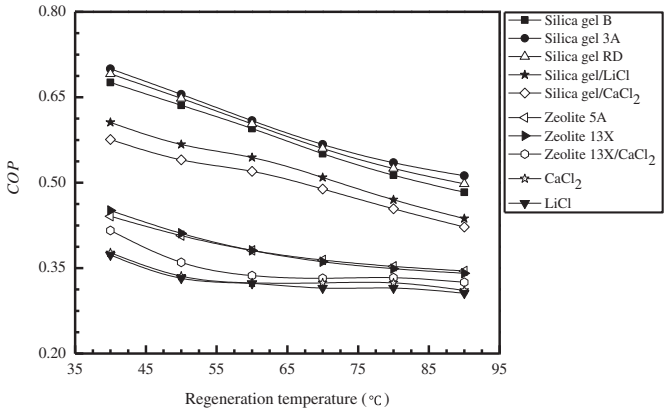

Fig. 8. Effects of regeneration temperature on *COP* under hot and dry operating conditions.

desiccants. Under humid conditions (ϕ = 85%), the equilibrium water content of desiccants approaches to the maximum equilibrium values. The equilibrium water content of zeolites 5A and 13X are the lowest, which results in low adsorption rates, and low dehumidification efficiency (ε_d) for these materials.

From analysis above, it can be concluded that silica gels 3A and RD are the best choices for air dehumidification under hot and humid operating conditions, based on the performances of *COP*, *SDP* and ε_d.

3.2.2. Hot and dry conditions

Calculated results for the *COP*, *SDP* and ε_d with different desiccant materials under hot and dry operating conditions are plotted in Figs. 8–10.

Fig. 8 shows that the *COP* decreases monotonically with regeneration temperature increasing. This is because the equilibrium water content in the desiccants at low relative humidity (20%) is lower than that at high relative humidity (85%). Energy consumption increases more quickly than useful energy output with increasing regenerating temperature under this operating condition. In addition, it is clear that the *COP*s of silica gels B, 3A and RD are always better than others at different regeneration temperatures.

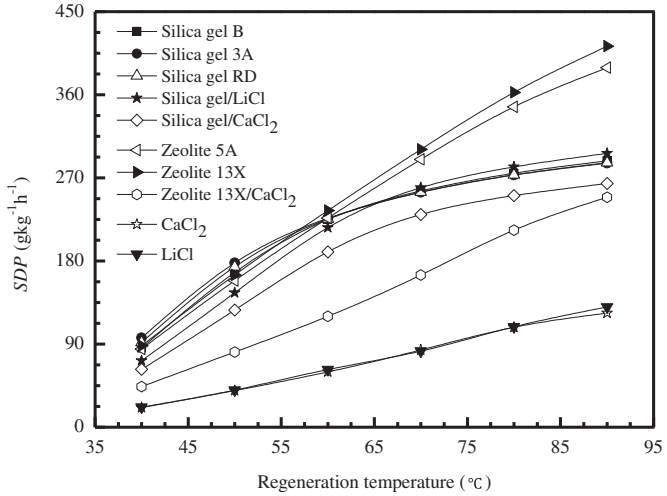

Fig. 9. Effects of regeneration temperature on *SDP* under hot and dry operating conditions.

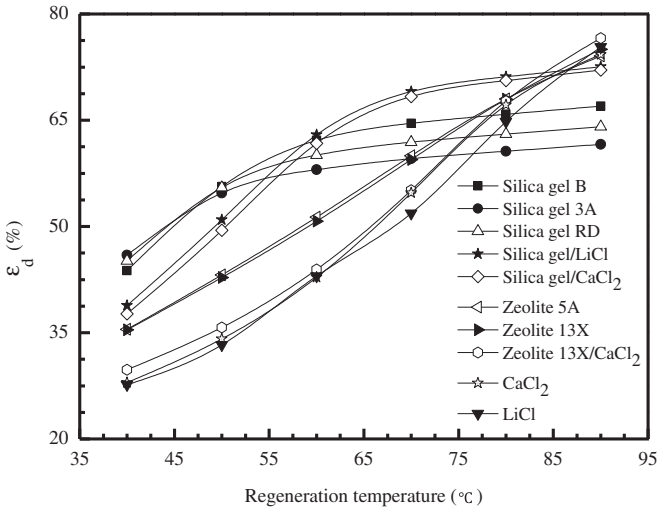

Fig. 10. Effects of regeneration temperature on ε_d under hot and dry operating conditions.

The variations of *SDP* with regeneration temperatures are shown in Fig. 9. Clearly, the *SDP*s of zeolites 13X and 5A increase steeply from 90 g kg^{-1} h^{-1} to 400 g kg^{-1} h^{-1} with increasing regeneration temperature when regeneration temperature is more than 60 °C, but at the same time the *SDP*s of other desiccants increase only slowly from 90 g kg^{-1} h^{-1} to 270 g kg^{-1} h^{-1}. This means that zeolites 13X and 5A are more sensitive to regeneration temperature than others do under hot and dry conditions. This is because the sorption curves for zeolites 5A and 13X are type I, which leads to the equilibrium water content in zeolites 5A and 13X larger than in others at low relative humidity (20%). Besides, the higher regeneration temperature results in a favorable effect on the desorption process for these two materials because of their larger adsorption heat (with values equal to 3974 kJ kg^{-1} and 3843 kJ kg^{-1}, respectively. They are 0.5 times larger than others). At the same time, it is found that the *SDP* of $CaCl_2$ and LiCl are only slightly increased with regeneration temperature increasing.

Fig. 10 shows that the ε_d increases monotonically with regeneration temperature increasing. It is found that the ε_d of silica gels B, 3A and RD is higher than others when the regeneration temperature is less than 50 °C, however the ε_d of silica gel/LiCl and silica gel/$CaCl_2$ is higher than others when the regeneration temperature is

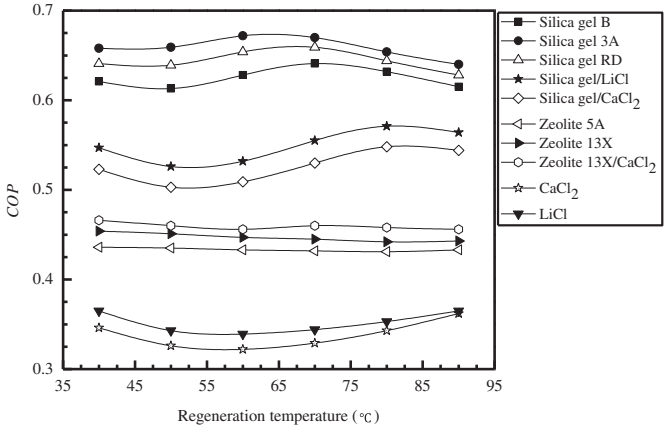

Fig. 11. Effects of regeneration temperature on *COP* under cool and humid operating conditions.

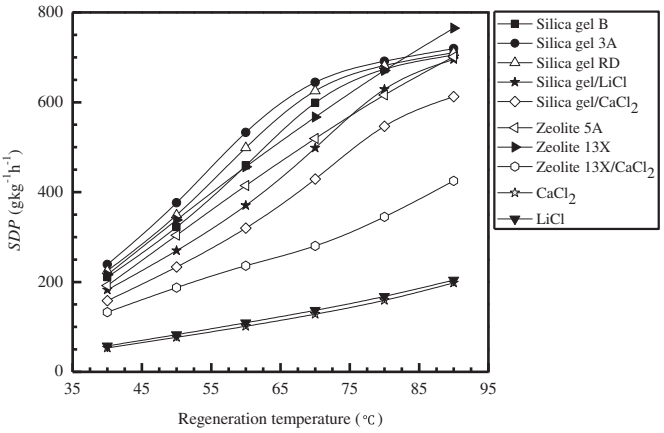

Fig. 12. Effects of regeneration temperature on *SDP* under cool and humid operating conditions.

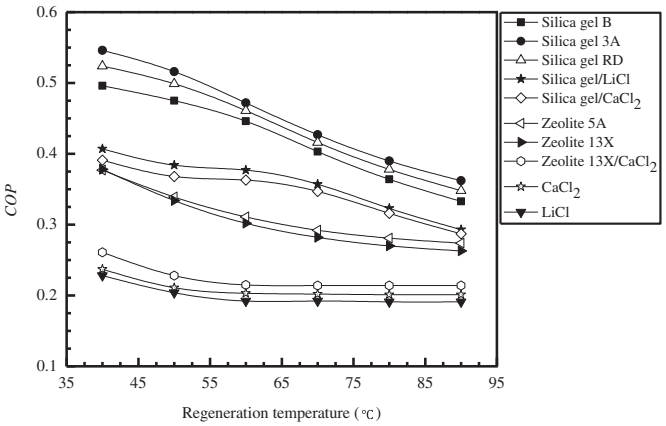

Fig. 14. Effects of regeneration temperature on *COP* under cool and dry operating conditions.

between 60 °C and 80 °C. In addition, it can be seen that the ε_d of zeolite 5A and 13X increases linearly with a higher regeneration temperature. It then reaches the highest value of 76% when the regeneration temperature reaches to 90 °C.

3.2.3. Cool and humid conditions

Calculated results for the *COP*, *SDP* and ε_d with different solid desiccants under cool and humid operating conditions are plotted in Figs. 11–13.

The *COP*s are nearly unchanged with regeneration temperature increasing as shown in Fig. 11. The trends are similar to the hot and humid operating conditions, but with lower *COP* values. These facts reveal that the *COP*s under high relative humidity are less influenced by regeneration temperature than those under low relative humidity.

The trends of *SDP* with regeneration temperature under cool and humid operating conditions for various solid desiccants are shown in Fig. 12. It is clear that the *SDP*s of most desiccants increase quickly with regeneration temperature increasing when the regeneration temperature is lower than 70 °C, but they increases only slightly when the regeneration temperature is higher than 70 °C. Further, the *SDP*s of zeolites 13X, 5A and silica gel/LiCl increase quickly when the regeneration temperature increases from 40 °C to 90 °C. These phenomena reveal that for zeolites 13X, 5A, and silica gel/LiCl composite, the higher the *SDP*s are, the larger the driven heat is needed.

The ε_d of various desiccants changes largely with regeneration temperature increasing as shown in Fig. 13. It can be seen that the ε_d of various desiccants is less than 30% when the regeneration temperature is 40 °C, while the ε_d of various desiccants is above 48% when the regeneration temperature is 90 °C. Further, it can be found that the ε_d of silica gels B, 3A and RD increases from 30% to 60% when the regeneration temperature increases from 40 °C to 70 °C. Consequently, the high dehumidification efficiency can be reached with low grade heat sources under cool and humid operating conditions.

3.2.4. Cool and dry conditions

Calculated results for the *COP*, *SDP* and ε_d with different desiccants under cool and dry operating conditions are plotted in Figs. 14–16.

From Fig. 14, we can see that the *COP*s are decreased slightly with regeneration temperature increasing. The *COP* values of silica gel 3A decrease from 0.55 to 0.38, while the *COP* values of LiCl decrease from 0.23 to 0.2. This means that the *COP*s of silica gel 3A are more sensitive to regeneration temperature than LiCl under

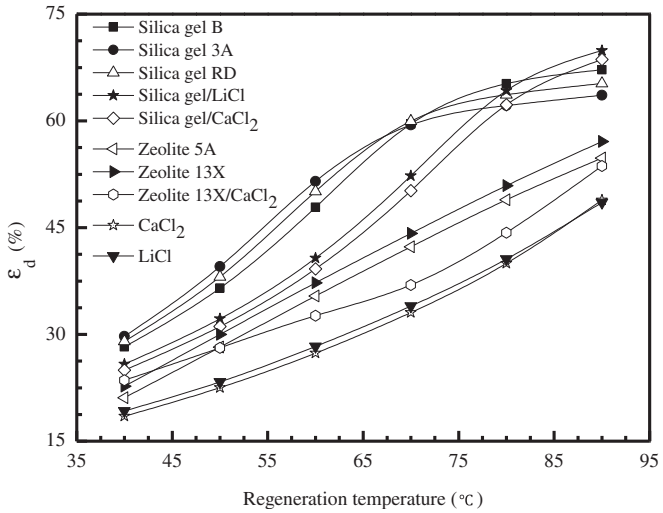

Fig. 13. Effects of regeneration temperature on ε_d under cool and humid operating conditions.

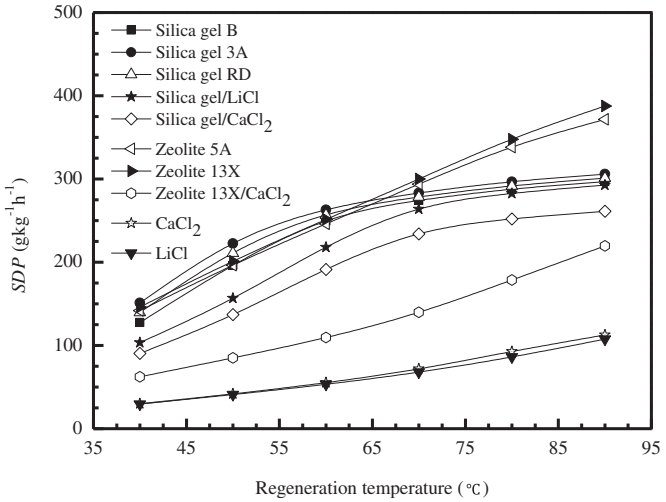

Fig. 15. Effects of regeneration temperature on *SDP* under cool and dry operating conditions.

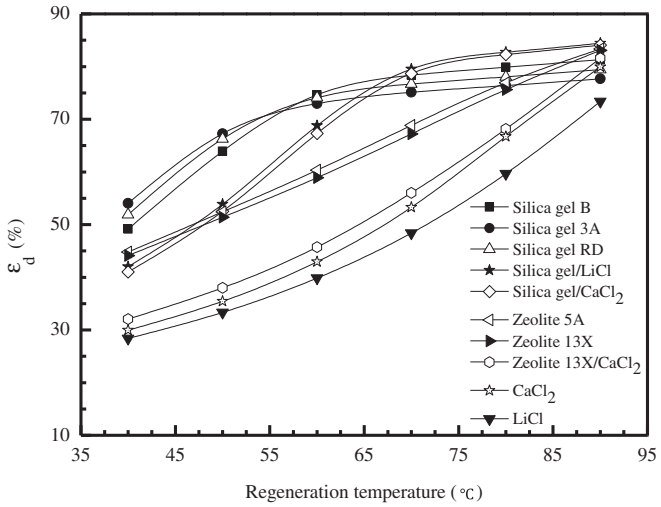

Fig. 16. Effects of regeneration temperature on ε_d under cool and dry operating conditions.

cool and dry operating conditions. This is mainly because the adsorption heat of silica gel 3A (with value equals to 2380 kJ kg^{-1}) is lower than that of LiCl (with value equals to 2957 kJ kg^{-1}).

The trends of *SDP*s with regeneration temperature under cool and dry operating conditions for various solid desiccants are shown in Fig. 15. The *SDP*s of zeolites 5A, 13X, and zeolite 13X/$CaCl_2$ composite increases linearly with a higher regeneration temperature, while the *SDP*s of LiCl and $CaCl_2$ only increase slightly. The *SDP*s of other desiccants increase linearly at first, and then tend to remain unchanged. Further, it can be seen that the *SDP* of zeolite 13X is nearly 100 g/kg/h higher than that of silica gel 3A when the regeneration temperature is 90 °C. However, in order to conserve energy, it is better to chose silica gels such as types B, 3A or RD as the dehumidification materials because they can be regenerative at lower temperatures.

From Fig. 16, it can be seen that the ε_d of silica gels B, 3A and RD is higher than other candidates when the regeneration temperature is less than 60 °C. However the ε_d of silica gel/LiCl composite and silica gel/$CaCl_2$ composite is higher than other desiccants when the regeneration temperature is between 70 °C and 90 °C. In addition, it is noticed that if the regeneration temperature is higher than 60 °C, the ε_d of silica gels B, 3A and RD changes little. It is noticed that 60 °C is within the working temperature range for the low grade waste heat [25]. Consequently, the adsorption beds fabricated with silica gels B, 3A and RD materials are suitable to be used in waste heat recovery under cool and dry operating conditions. These materials are also ideal candidates for other operating conditions if driven by low grade waste heat.

4. Conclusions

In this paper, the performances of air dehumidification with cycling honeycomb desiccant adsorption beds are analyzed with a one-dimensional transient heat and mass transfer model. Totally 10 kinds of desiccants are considered. One material is fabricated in our laboratory and used for model validation. Other 9 are taken from references and are selected for performance comparisons. They are modeled from the point of view of "system operation", rather than from "raw materials". The main conclusions can be summarized as follows:

(1) The *COP*s of various solid desiccants tend to remain unchanged with a higher regeneration temperature under humid operating conditions, but they decrease with regeneration temperature increasing under dry operating conditions.
(2) Both the *SDP* and the ε_d of various solid desiccants increase monotonically with a higher regeneration temperature, under all four operating conditions.
(3) Of the various desiccants, the silica gels B, 3A and RD always perform better than other candidates for air dehumidification under most operating conditions, when low grade waste heat is used as the driving energy.
(4) When driven by low grade waste heat (40–60 °C), the order for the selection of materials should be:

For all four operating conditions

COP and ε_d: silica gel 3A > silica gel RD > silica gel B > silica gel/LiCl > silica gel/$CaCl_2$

Hot and humid operating conditions

SDP: silica gel 3A > silica gel RD > silica gel B > silica gel/LiCl > silica gel/$CaCl_2$

Hot and dry operating conditions

SDP: silica gel 3A > silica gel RD > silica gel B > zeolite 13X > zeolite 5A

Cool and humid operating conditions

SDP: silica gel 3A > silica gel RD > zeolite 13X > silica gel B > zeolite 5A

Cool and dry operating conditions

SDP: silica gel 3A > silica gel RD > zeolite 13X > zeolite 5A > silica gel B

Acknowledgments

This project is supported by Natural Science Foundation of China, No. 51376064.

References

[1] Zhang LZ, Niu JL. Energy requirements for conditioning fresh air and the longterm savings with a membrane-based energy recovery ventilator in Hong Kong. Energy 2001;26:119–35.
[2] Zhang LZ. Energy performance of independent air dehumidification systems with energy recovery measures. Energy 2006;31:1228–42.
[3] Zhang LZ. Heat and mass transfer in plate-fin enthalpy exchangers with different plate and fin materials. Int J Heat Mass Transf 2009;52:2704–13.
[4] Nakabayashi S, Nagano K, Nakamura M, Togawa J, Kurokawa A. Improvement of water vapor adsorption ability of natural mesoporous material by impregnating with chloride salts for development of a new desiccant filter. Adsorption 2011;17:675–86.
[5] Liang CH, Zhang LZ, Pei LX. Performance analysis of a direct expansion air dehumidification system combined with membrane-based total heat recovery. Energy 2010;35:3891–901.
[6] Ng KC, Chua HT, Chung CY, Loke CH, Kashiwagi T, Akisawa A, et al. Experimental investigation of the silica gel-water adsorption isotherm characteristics. Appl Therm Eng 2001;21:1631–42.
[7] Tashiro Y, Kubo M, Katsumi Y, Meguro T, Komeya K. Assessment of adsorption-desorption characteristics of adsorbents for adsorptive desiccant cooling system. J Mater Sci 2004;39:1315–9.
[8] Zhang XJ, Sumathy K, Dai YJ, Wang RZ. Parametric study on the silica gel-calcium chloride composite desiccant rotary wheel employing fractal BET adsorption isotherm. Int J Energy Res 2005;29:37–51.
[9] Chan KC, Chao CYH, Sze-To GN, Hui KS. Performance predictions for a new zeolite 13X/$CaCl_2$ composite adsorbent for adsorption cooling systems. Int J Heat Mass Transf 2012;55:3214–24.
[10] Yadav A, Bajpai VK. Experimental comparison of various solid desiccants for regeneration by evacuated solar air collector and air dehumidification. Drying Technol 2012;30:516–25.
[11] Jia CX, Dai YJ, Wu JY, Wang RZ. Experimental comparison of two honeycombed desiccant wheels fabricated with silica gel and composite desiccant material. Energy Convers Manag 2006;47:2523–34.
[12] Liu YF, Wang RZ. Pore structure of new composite adsorbent $SiO_2 \cdot xH_2O \cdot yCaCl_2$ with high uptake of water from air. Sci China (Series E) 2003;46:551–9.
[13] Zhang LZ. Conjugate heat mass transfer in heat mass exchanger ducts. New York: Acedemic Press, Elsevier; 2013.
[14] Zhang LZ. Total heat recovery: heat and moisture recovery from ventilation air. New York: Nova Science Publishers, Inc; 2009.

[15] Zhang LZ, Niu JL. Performance comparisons of desiccant wheels for air dehumidification and enthalpy recovery. Appl Therm Eng 2002;22:1347–67.
[16] Pesaran AA, Mills AF. Moisture transport in silica gel packed beds. I-theoretical study. Int J Heat Mass Transf 1987;30:1037–49.
[17] Zhang LZ. Evaluation of moisture diffusivity in hydrophilic polymer membranes: a new approach. J Membr Sci 2006;269:75–83.
[18] Zhang LZ, Wang L. Performance estimation of an adsorption cooling system for automobile waste heat recovery. Appl Therm Eng 1997;17:1127–39.
[19] La D, Li Y, Dai YJ, Ge TS, Wang RZ. Development of a novel rotary desiccant cooling cycle with isothermal dehumidification and regenerative evaporative cooling using thermodynamic analysis method. Energy 2012;44:778–91.
[20] Jia CX, Dai YJ, Wu JY, Wang RZ. Use of compound desiccant to develop high performance desiccant cooling system. Int J Refrig 2007;30:345–53.
[21] Aristov YI, Restuccia G, Cacciola G, Tokarev MM. Selective water sorbents for multiple applications, 7. heat conductivity of $CaCl_2$-SiO_2 composites. React Kinet Catal Lett 1998;65:277–84.
[22] Aristov YI, Restuccia G, Tokarev MM, Cacciola G. Selective water sorbents for multiple applications, 10. energy storage ability. React Kinet Catal Lett 2000;69:345–53.
[23] Chen HJ, Cui Q, Tang Y, Chen XJ, Yao HQ. Attapulgite based LiCl composite adsorbents for cooling and air conditioning applications. Appl Therm Eng 2008;28:2187–93.
[24] Patnaik P. Handbook of inorganic chemicals. New York: McGraw-Hill; 2003.
[25] Tso CY, Chao CYH, Fu SC. Performance analysis of a waste heat driven activated carbon based composite adsorbent-water adsorption chiller using simulation model. Int J Heat Mass Transf 2012;55:7596–610.